The Role of Sea-Swell, Infragravity Waves, and Dune Geometry on Runup Excursion During Dune Collision

Christine M. Baker[1,2(✉)], Katherine Anarde[2], Marion Tissier[3], Jantien Rutten[3,4], Paul van Wiechen[3], Ryan Mieras[5], and Sierd De Vries[3]

[1] Stanford University, Stanford, CA 94305, USA
bakercm@stanford.edu
[2] North Carolina State University, Raleigh, NC 27606, USA
[3] Delft University of Technology, Mekelweg 5, 2628 CD Delft, Netherlands
[4] Boussinesqweg 1, 2629 HV Delft, Netherlands
[5] University of North Carolina Wilmington, Wilmington, NC 28403, USA

Abstract. Storm-elevated water levels can lead to waves attacking the dune face (dune collision regime), resulting in avalanching and shoreward translation of the dune face. Predicting dune erosion rates during storms is critical, yet, our knowledge of the relative role of infragravity and sea-swell waves on runup excursion on an eroding dune face relies primarily on numerical modeling. Here, we assess the role of sea-swell waves, infragravity waves, and dune geometry on runup excursion during dune collision with observations collected during the Realdune/REFLEX field experiment. In situ and lidar observations were collected from Oct. 2021 to Jan. 2022 at the Sand Engine in the Netherlands. Incident sea-swell and infragravity wave contributions resulting in runup on an artificial, unvegetated dune during two winter storms were quantified. We find that infragravity wave crests contributed to the largest runup events on the dune. Additionally, runup excursion is modified by dune geometry, where more sediment at the dune base, associated with a relatively mild dune face, reduced runup extent relative to events with steeper dune faces. This suggests that shallower dune geometries with more sand at the base may temporarily enhance dune safety by reducing runup.

Keywords: Storm events · infragravity waves · dune collision · runup excursion · lidar

1 Introduction

Storm-elevated water levels can result in waves attacking the dune face, leading to significant dune erosion. Continuous incident swash that runs up the dune face but does not exceed the dune crest, known as the 'dune collision regime' [1], can lead to dune steepening and subsequent slumping events [2–4]. This process redistributes sediment from the dune face to its base [5], where it can be subsequently transported offshore, resulting in shoreward translation of the dune [6]. When mean water levels remain

C. Coelho et al. (Eds.): CD 2025, COASTALRL 42, pp. 37–42, 2026.
https://doi.org/10.1007/978-3-032-15477-4_7

below the dune toe during dune collision, instantaneous wave activity dictates the runup excursions on the dune face. Consequently, wave-by-wave processes, which encompass infragravity and sea-swell wave forcing, control dune erosion rates during this stage. During storms, infragravity waves often dominate inner surf dynamics [7] and may be a primary offshore transport mechanism of sand from the dune [8]. Yet, our knowledge of the role of infragravity and sea-swell waves on runup excursion for an actively eroding dune face is primarily informed by numerical modeling studies (e.g., [9]), with few field observations to test our mechanistic understanding. Here, we address this data and knowledge gap by relating observations of incident wave-by-wave characteristics and dune geometry to runup excursions at an artificial, unvegetated dune during two winter storms (Fig. 1).

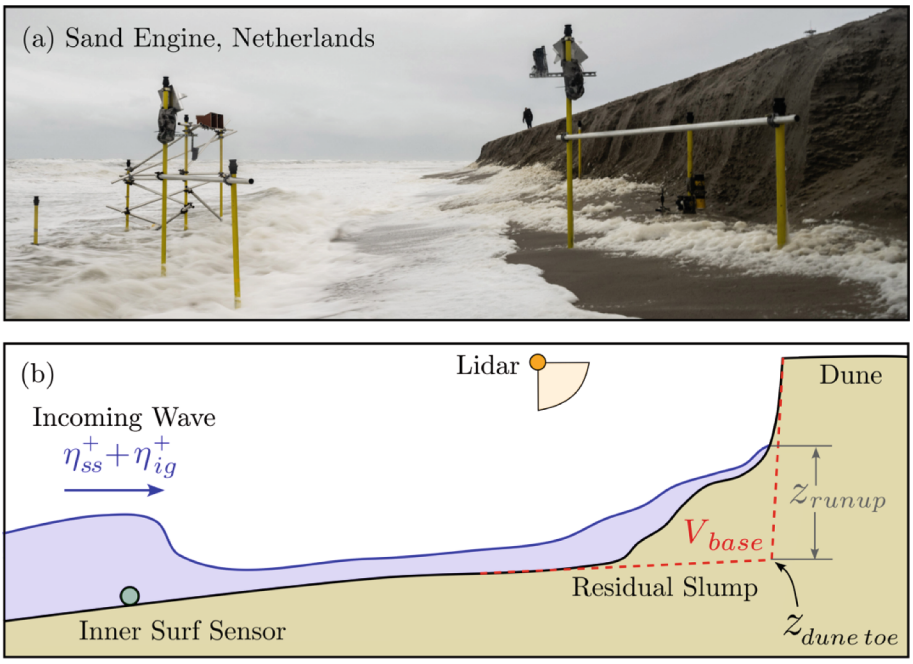

Fig. 1 (a) An image of the field site and instrumentation during elevated water levels. (b) A schematic of the dune with a volume of sand at its base (V_{base}) that is overtopped by runup with an excursion height on the dune (z_{runup}), and an incoming wave with an amplitude composed of infragravity (η_{ig}^{+}) and sea-swell (η_{ss}^{+}) wave components.

2 Storm Observations

Hydro- and morphodynamic data were collected at the Sand Engine along the Dutch coast during the Realdune/REFLEX Experiment (Oct. 2021 - Jan. 2022; [10, 11]). Two artificial, unvegetated dunes were constructed just above the high-water line, increasing

the likelihood of dune collision during winter storm events (Fig. 1a). Cross-shore arrays of in situ sensors measuring pressures and velocities were deployed in the inner surf and swash zone at both dunes. The runup elevation and dune geometry at the southern dune were estimated from 6-Hz continuous cross-shore lidar scans (Fig. 1b). Incoming storm wave conditions and water levels were measured in 14-m water depth [11].

Here, we characterize storm processes at the southern dune during two storms with elevated water levels ($\langle\eta\rangle = 2.07$ m and 2.38 m) and large shore-normal and oblique waves ($H_s = 3.12$ m and 3.48 m). Bulk incident infragravity wave energy and reflection coefficients in the inner surf zone remained relatively stationary through each event. Dune collision occurred during both storms, resulting in significant net erosion of the dune face (December event: 2 m3/m, January event: 9 m3/m, Fig. 2a). [4] showed that dune erosion rates throughout both storms were correlated with the total water level (i.e., the mean water level plus individual waves) with the shortest time between slumps occurring during increasing water levels (Fig. 2b). Notably, however, mean water levels did not exceed the dune toe during either event. As a result, runup excursions on the dune face were driven by individual waves (Fig. 2c).

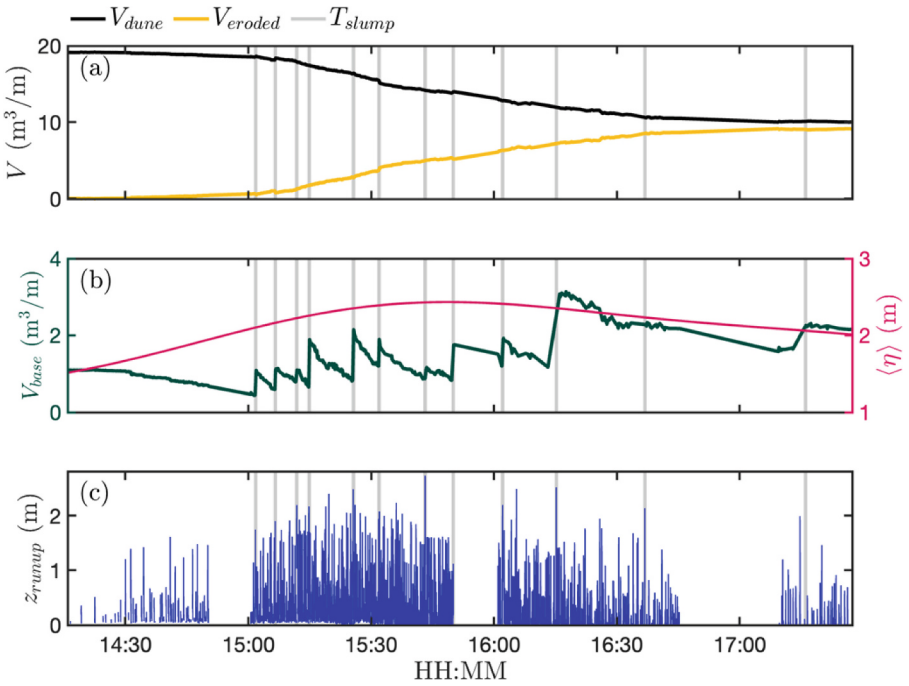

Fig. 2. Hydro- and morphodynamic time series over the January storm event, including (a) the dune volume (V_{dune}, , black) and volumed eroded from the dune (V_{eroded}, , gold), (b) the volume at the base of the dune (V_{base}, , teal) and mean water level at the inner surf zone sensor ($\langle\eta\rangle$, , pink), (c) the runup excursion elevation above the dune toe (z_{runup}). The time of slumping events (T_{slump}) are shown as vertical grey bars (as identified by [4]).

3 Determining Wave-By-Wave Characteristics

We investigate the relationships between incoming infragravity and sea-swell waves, dune geometry, and runup during each collision (Fig. 2). The runup excursion elevation (z_{twl}, defined relative to the dune toe, Fig. 2c) and the remaining volume of the previous slump in front of the dune (V_{base}, Fig. 2b, [10]) were computed from 4-Hz filtered lidar profiles. The incident waves in the inner surf zone were quantified with co-located pressure and velocity sensors [12] and band-passed to isolate the infragravity (η_{ig}^{+}, $0.004 < f < 0.04$ Hz) and sea-swell ($\eta_{ss}^{+}, f > 0.04$ Hz) wave amplitudes (Fig. 3c,d). The wave-by-wave runup excursion height on the dune ($z_{runup} = z_{twl,max} - z_{dunetoe}$) was characterized as the maximum runup elevation during a continuous time series of total water levels exceeding 0.1 m above the dune toe ($z_{dunetoe}$). The incoming wave associated with a runup event was identified as the maximum total incoming wave amplitude ($\eta_{ss}^{+} + \eta_{ig}^{+}$) that propagated past the inner surf zone station 3 to 8 s prior to a runup event, which was informed by estimating bore speeds (Fig. 3a,b).

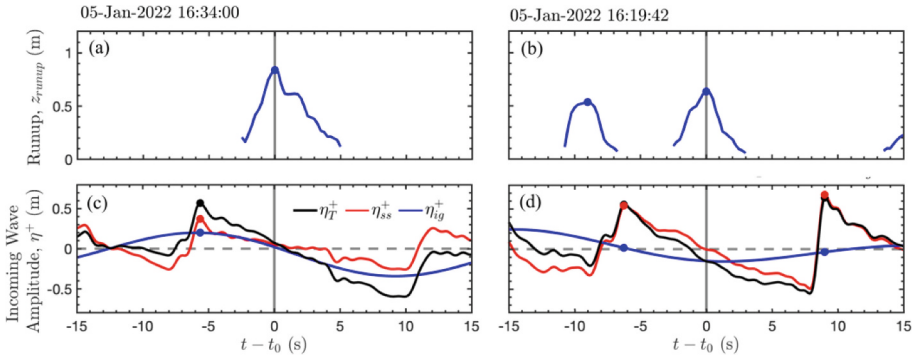

Fig. 3. Example time series of (a,b) the runup height (z_{runup}) above the dune toe and (c,d) the incoming total (η_T^+, , black), sea-swell (η_{ss}^+, , red), and infragravity (η_{ig}^+, , blue) wave amplitude, centered at the maximum runup excursions during events with (a,c) significant and (b,d) no contribution from an infragravity wave crest.

4 Runup Excursion Drivers

The runup excursion heights generally increased with total incoming wave amplitudes but with significant scatter (Fig. 4a). Nearly all runup events were partially associated with an incoming sea-swell wave crest at the inner surf-zone sensor ($\eta_{ss}^{+} > 0$ m, Fig. 3 and 4b), but not necessarily by an infragravity wave crest ($\eta_{ig}^{+} > 0$ m, Fig. 3b,d and Fig. 4c). Occasionally, runup events occurred in infragravity wave troughs ($\eta_{ig}^{+} < 0$ m). However, the 90th percentile largest runup excursions ($z_{runup} \geq 1.75$ m) nearly always included contributions from both infragravity and sea-swell wave crests. Sea-swell waves may dissipate energy between the inner surf zone and the dune; however, the dissipation of incident infragravity wave energy between these sampling locations is expected to be minimal [13]. Still, this suggests that both sea-swell and infragravity waves are important

in determining runup at the dune that may suspend and advect sediment offshore. Dune geometry also alters runup excursion heights. For a given incoming wave amplitude, the volume of the previous slump in front of the dune reduced the runup excursion height. Thus, we find that relatively mild dune slopes, when more sand is at the base (larger V_{base}), may temporarily enhance dune safety by reducing runup.

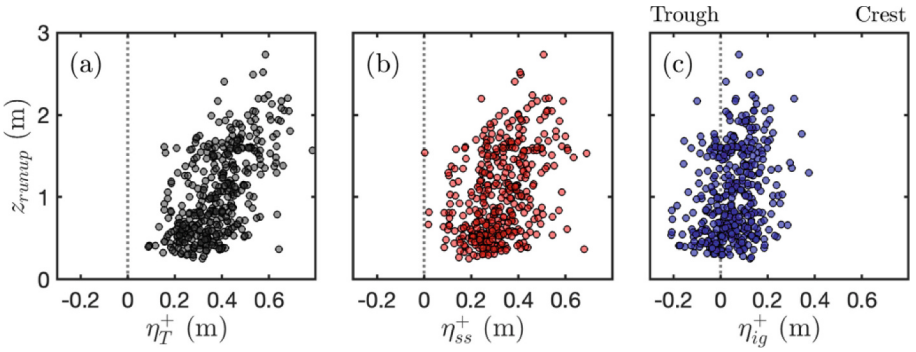

Fig. 4. Runup excursion height on the dune (z_{runup}) vs. the associated incoming (a) total (η_T^+), (b) sea-swell (η_{ss}^+), and (c) infragravity (η_{ig}^+) wave amplitude.

5 Conclusion

The role of infragravity waves, sea-swell waves, and dune geometry during dune collision were investigated with field observations during two winter storms. Runup events on the artificial dune, extracted from lidar measurements, were driven by waves, as the mean water level remained below the dune toe throughout the storms. Wave-by-wave runup excursion on the dune was related to the infragravity and sea-swell incoming wave amplitude driving the event. Infragravity waves contributed to the largest runup events on the dune; however, some runup events occurred independently of an infragravity wave crest. A smaller volume of sand at the base of the dune, associated with a steeper dune slope, often resulted in higher runup excursion on the dune. Our findings further emphasize the need for a rigorous understanding of infragravity and sea-swell wave transformation to predict dune erosion rates during the dune collision regime.

References

1. Sallenger AH Jr (2000) Storm impact scale for barrier islands. J Coastal Res 16(3):890–895
2. Van Bemmelen CWT, De Schipper MA, Darnall J, Aarninkhof SGJ (2020) Beach scarp dynamics at nourished beaches. Coast Eng 160:103725
3. Van Gent MRA, de Vries JVT, Coeveld EM, De Vroeg JH, Van de Graaff J (2008) Large-scale dune erosion tests to study the influence of wave periods. Coast Eng 55(12):1041–1051
4. van Wiechen P, Mieras R, Tissier M, de Vries S (2024) Coastal dune erosion and slumping processes in the collision regime based on field measurements. J Geophy Res Earth Surface 129(10)

5. Erikson LH, Larson M, Hanson H (2007) Laboratory investigation of beach scarp and dune recession due to notching and subsequent failure. Mar Geol 245(1–4):1–19
6. Castelle B, et al (2015) Impact of the winter 2013–2014 series of severe Western Europe storms on a double-barred sandy coast: Beach and dune erosion and megacusp embayments. Geomorphology 238: 135–148
7. Raubenheimer B, Guza RT, Elgar S (1996) Wave transformation across the inner surf zone. J Geophy Res: Oceans 101(C11):25589–25597
8. Roelvink D, Reniers A, Van Dongeren AP, De Vries JVT, McCall R, Lescinski J (2009) Modeling storm impacts on beaches, dunes and barrier islands. Coast Eng 56(11–12):1133–11552
9. McCall RT et al (2010) Two-dimensional time dependent hurricane overwash and erosion modeling at Santa Rosa Island. Coast Eng 57(7):668–683
10. van Wiechen P et al (2024) Measurements of dune erosion processes during the Real-Dune/REFLEX experiments. Scientific Data 11(1):421
11. Rutten J et al (2024) Continuous wave measurements collected in intermediate depth throughout the north sea storm season during the realdune/reflex experiments. Data 9(5):70
12. Guza RT, Thornton EB, Holman RA (1984) Swash on steep and shallow beaches. In: Proceedings of the 19th International Conference on Coastal Engineering, pp. 708–723. ASCE
13. De Bakker ATM, Herbers THC, Smit PB, Tissier MFS, Ruessink BG (2015) Nonlinear infragravity–wave interactions on a gently sloping laboratory beach. J Phys Oceanogr 45(2):589–605